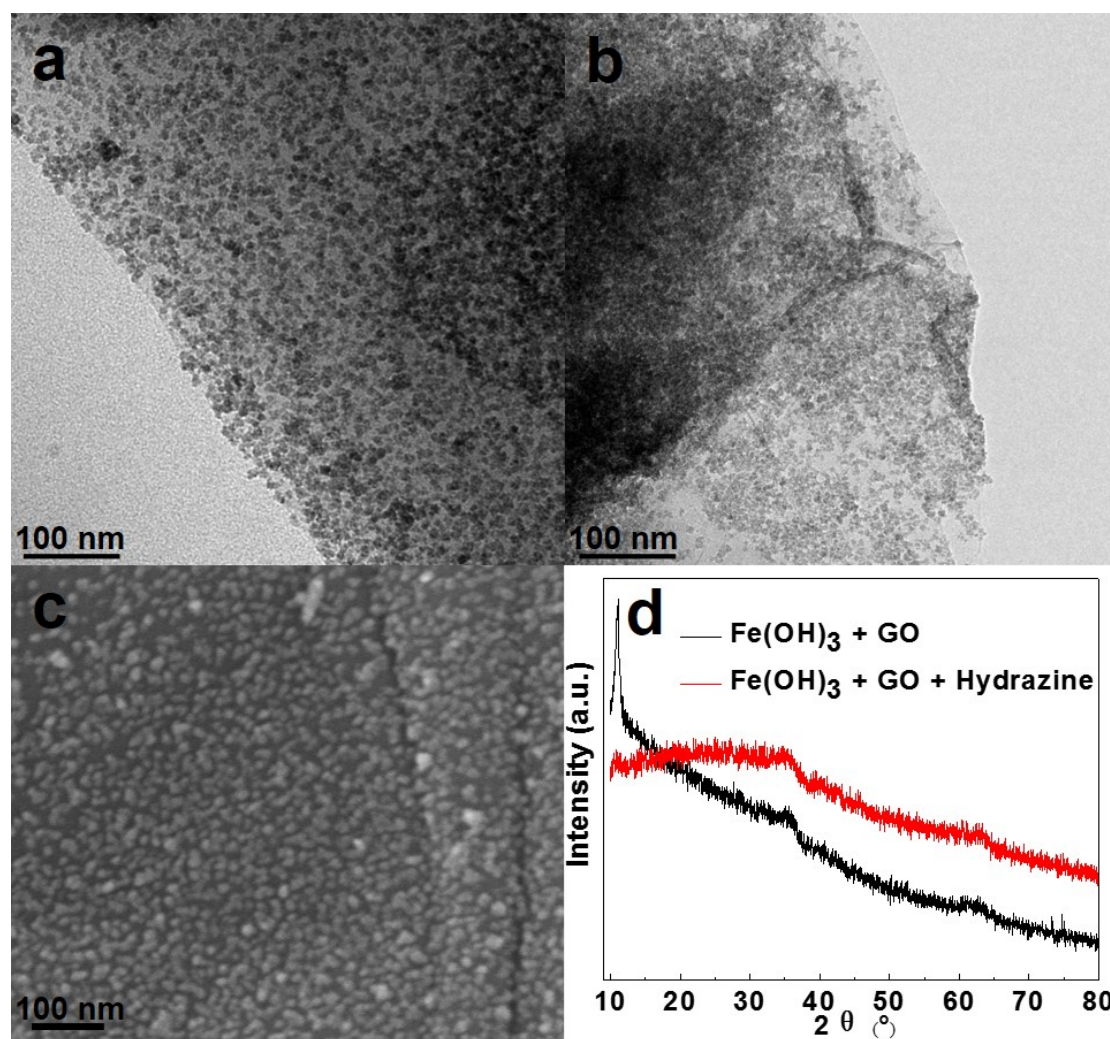
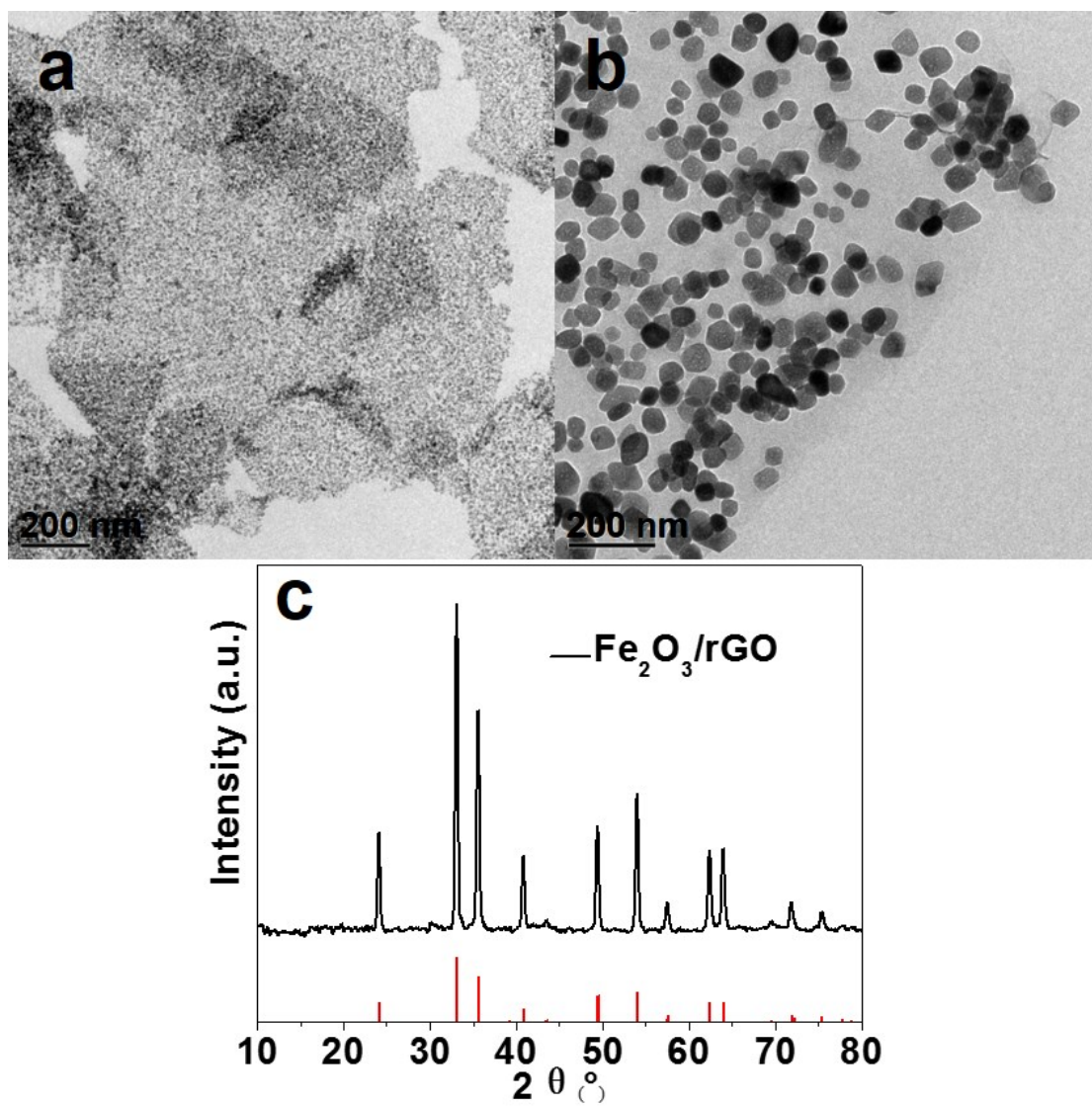


### Supporting Information



**Figure S1.** TEM images of Fe(OH)<sub>3</sub>/GO obtained by mixing Fe(OH)<sub>3</sub> sol and GO solution with (a) or without (b) adding hydrazine. (c) SEM image of the above Fe(OH)<sub>3</sub>/GO with adding hydrazine. (d) XRD patterns of the Fe(OH)<sub>3</sub>/GO and Fe(OH)<sub>3</sub>/GO after adding hydrazine.



**Figure S2.** TEM images of Fe<sub>3</sub>O<sub>4</sub>/rGO-180 (a) and Fe<sub>2</sub>O<sub>3</sub>/rGO (b), and XRD pattern of Fe<sub>2</sub>O<sub>3</sub>/rGO (c). Fe<sub>2</sub>O<sub>3</sub>/rGO was obtained from hydrothermal reaction with Fe(OH)<sub>3</sub>, GO as precursors and hydrazine as reductants.

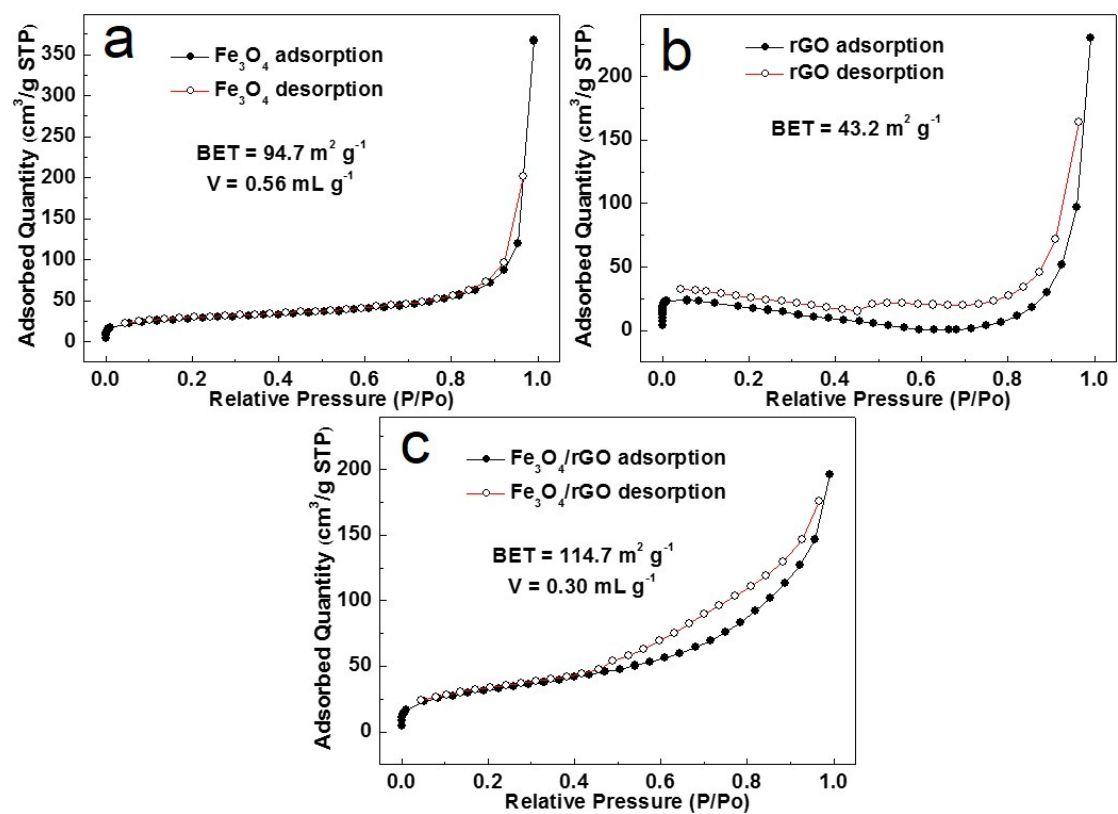


**Figure S3.** BET surface area of  $\text{Fe}_3\text{O}_4$ , rGO and  $\text{Fe}_3\text{O}_4/\text{rGO}$ .

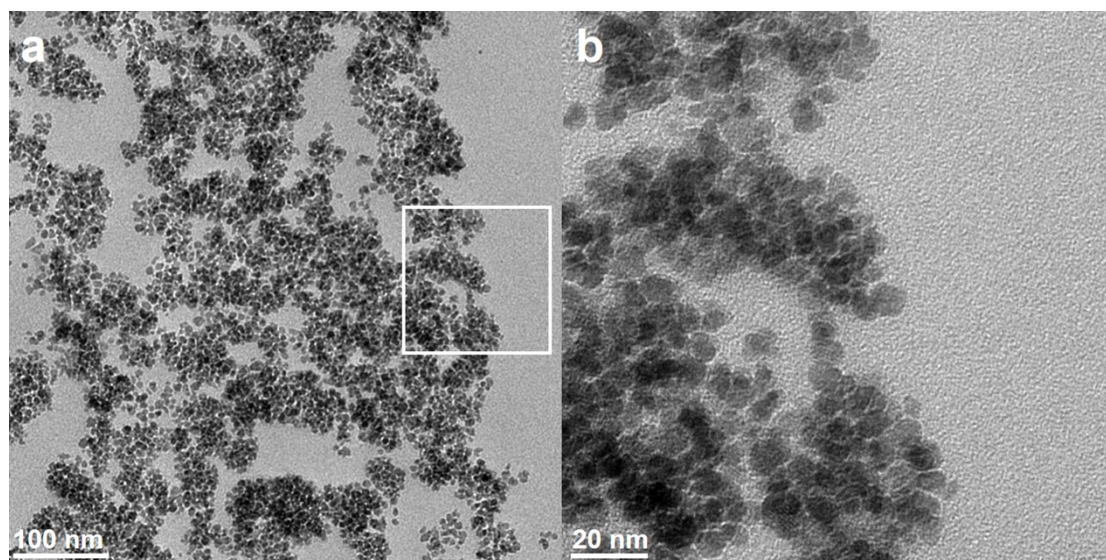


**Figure S4.** TEM images of  $\text{Fe}_3\text{O}_4$  nanoparticles at different magnifications.  $\text{Fe}_3\text{O}_4$  was obtained from hydrothermal reaction using  $\text{Fe}(\text{OH})_3$  as precursors, and VC and hydrazine as reductants.



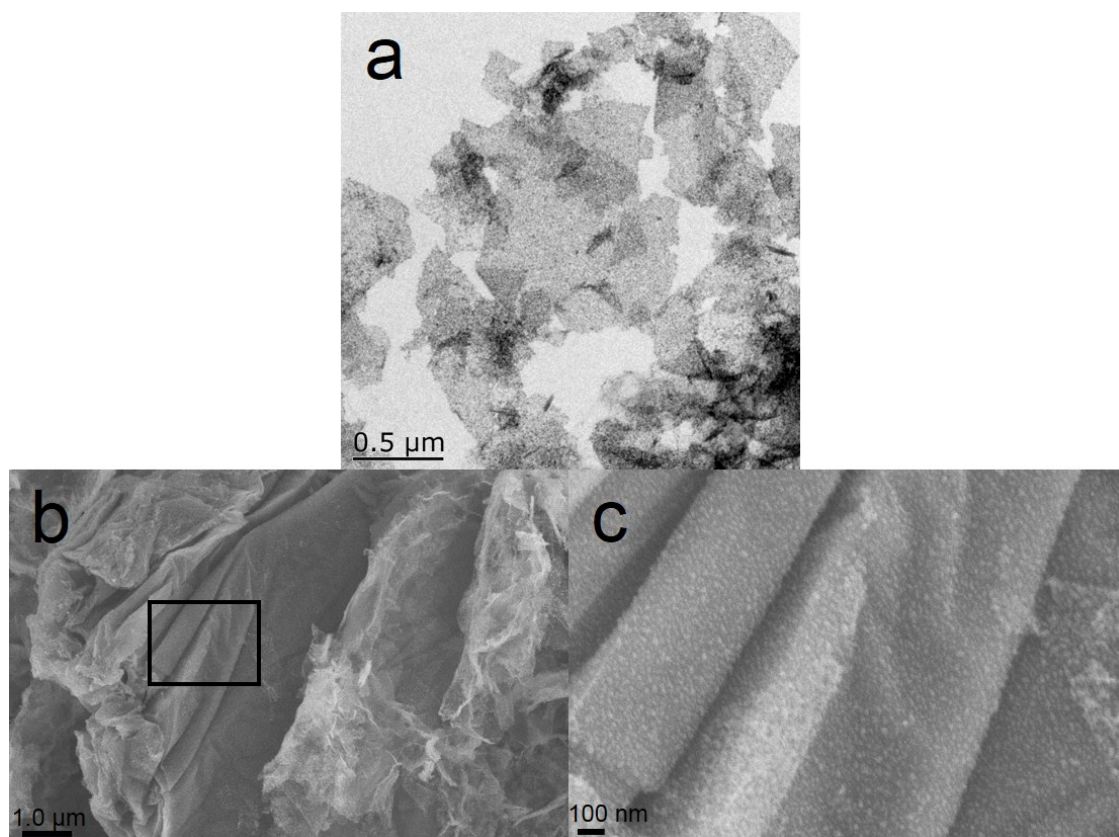


**Figure S5.** (a) TEM images of  $\text{Fe}_3\text{O}_4/\text{rGO}$ -180. (b and c) SEM images of  $\text{Fe}_3\text{O}_4/\text{rGO}$  at different magnifications.

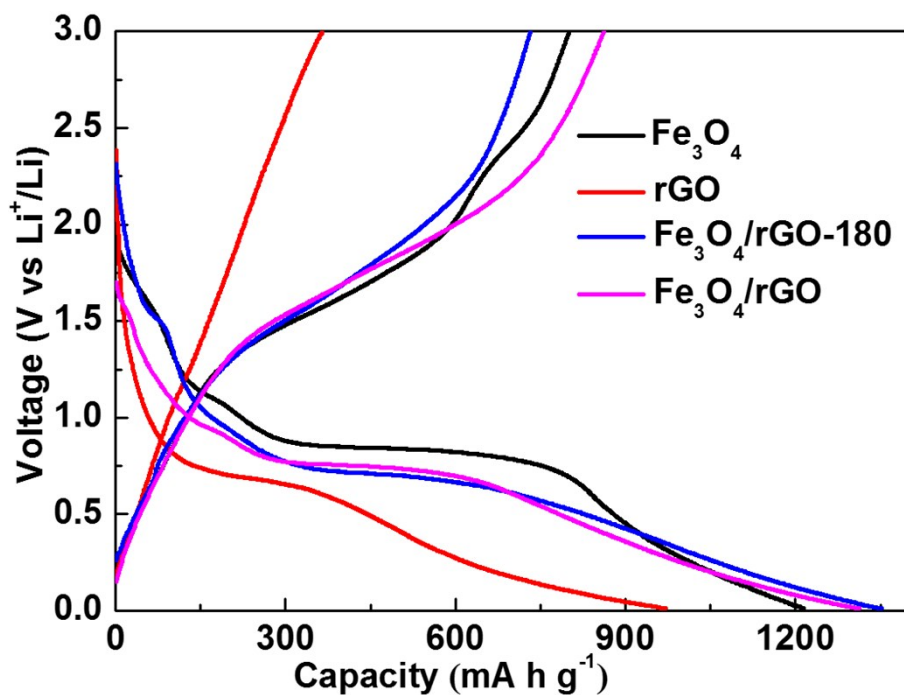


**Figure S6.** The first cycle charge-discharge profiles of cells with  $\text{Fe}_3\text{O}_4$ , rGO,  $\text{Fe}_3\text{O}_4/\text{rGO-180}$  or  $\text{Fe}_3\text{O}_4/\text{rGO}$ .

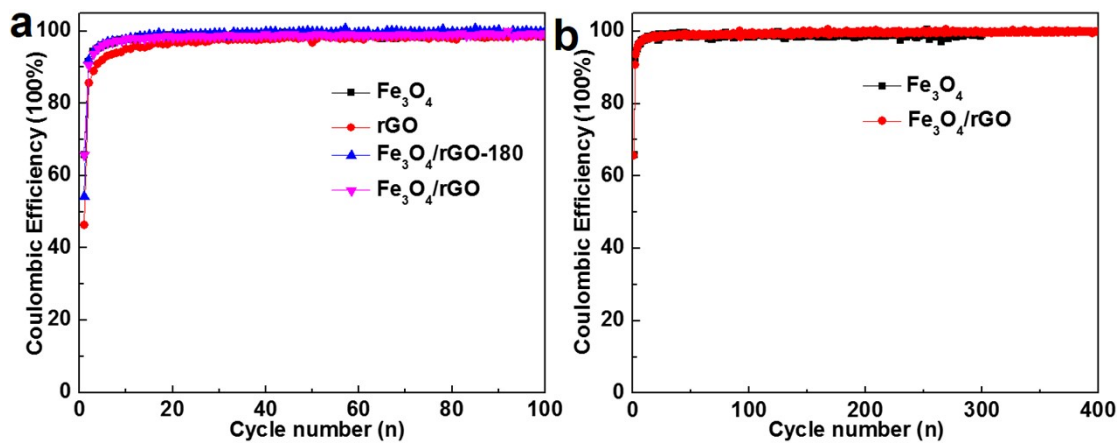


**Figure S7.** (a) Coulombic efficiencies of cells with rGO,  $\text{Fe}_3\text{O}_4$ ,  $\text{Fe}_3\text{O}_4/\text{rGO-180}$  or  $\text{Fe}_3\text{O}_4/\text{rGO}$  at a current density of  $0.5 \text{ A g}^{-1}$ . (b) Long-term charge-discharge Coulombic efficiencies of cells with  $\text{Fe}_3\text{O}_4$  or  $\text{Fe}_3\text{O}_4/\text{rGO}$ .

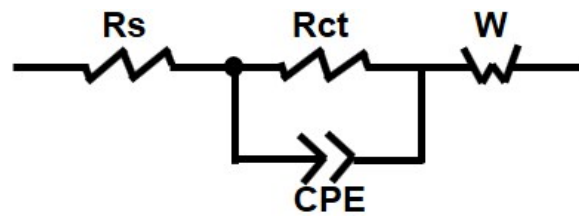


**Figure S8.** The equivalent circuit used for fitting cell resistances.